Appl Magn Reson (2016) 47:701–710
DOI 10.1007/s00723-016-0770-z

Applied
Magnetic Resonance

Decoherence-Induced Stabilization of the Multiple-Quantum NMR-Spectrum Width

A. A. Lundin[1] · **V. E. Zobov**[2]

Received: 24 June 2015 / Revised: 1 February 2016 / Published online: 20 February 2016

Abstract The time dependence of an increase in the number of correlated spins in cluster was calculated for a particular variant of multiple-quantum (MQ) nuclear magnetic resonance spectroscopy using an effective two-quantum Hamiltonian that includes conventional secular nuclear dipole–dipole interaction as a weak perturbation at the stage of correlation preparation. It was shown that the cluster size grows steadily, while the width of the MQ spectrum stabilizes because the decay rates of the spectral components located at different areas of the MQ spectrum are different. The MQ bandwidth was also calculated as a function of the preparation time for various perturbation strengths. The results obtained are in excellent agreement with the experimental data reported in Álvarez and Suter (Phys Rev A 84:012320, 2011).

1 Introduction

A multiple-quantum (MQ) solid-state nuclear magnetic resonance (NMR) is a powerful tool for the experimental study of many-particle systems connected by the natural or specifically designed interactions and specific interactions as well as for the precise control of the nuclear-spin dynamics [1–3]. The spin-system states arising in the MQ spectroscopy and developing under the action of certain

✉ V. E. Zobov
rsa@iph.krasn.ru

A. A. Lundin
andylun@orc.ru

[1] Semenov Institute of Chemical Physics, Russian Academy of Sciences, ul. Kosygina 4, Moscow 117977, Russia

[2] Kirensky Institute of Physics, Russian Academy of Sciences, Siberian Branch, Krasnoyarsk 660036, Russia

radio frequency (rf) pulse sequences are called multiple-spin coherences (or MQ coherences, depending on the experimental conditions). They are described by the many-particle time-correlation functions (TCFs) of a rather complicated form. The coherences and their dynamics provide great and, in some cases, unique possibilities in the study of particle behavior in different systems, such as particle clustering, formation of local structures on the surfaces, in liquid crystals, in nanocavities, etc. [4–6].

The processes of origination and decay of many-particle spin-correlations in quantum systems are of great importance in the development of modern methods of quantum-information processing and quantum computations [7]. The coherences prepared in a subsystem of nuclear spins can be controlled by the rf pulses to initiate the required processes.

Also, the methods of MQ spectroscopy are unique in that they provide a possibility for the experimental study of the processes of many-particle (many-spin) correlation preparation in the spin systems [8–13]. The high-order TCFs are used to describe the processes of monitoring quantum register with the aim to realize in practice the vast potentialities of quantum computers. The accuracy of monitoring must be increased with increasing number of qubits (spins) in the system, because the side relaxation processes can destroy the quantum-mechanical superposition in large clusters and render them more "fragile".

It was experimentally demonstrated in [8–13] that the number of dynamically correlated spins grows exponentially with time [14, 15]. With the parameter $a_0 \sim 0.01\ \mu s^{-1}$ corresponding to adamantane or to the CaF_2 crystal placed in a magnetic field directed along the [111] axis [15, 16], the number of dynamically correlated spins achieves a value of $\exp(a_0 t) \sim 10^{23}$ in a time of ~ 0.01 s, so that the whole crystal becomes a dynamically correlated cluster. It should be noted that the exponential growth with time was explained in [14] for the correlations only in ideal systems. In real systems, the exponential growth should eventually break down under the action of various perturbing factors such as spin–lattice relaxation, instrumental imperfections, etc. In this work, we do not discuss the possible causes for the correlation-growth breakdown, but are focused on the explanation of the experimental results reported in [11–13].

The possible reasons for the deviation from the exponential growth were discussed in [11–13]. It was assumed in [11–13] that the Anderson-like localization of dynamic correlations occurs in the nuclear spin system subjected to a weak perturbation [11–13, 17]. Nevertheless, we have recently argued [18] that the experimental method used in [11–13] is the main cause for the termination of the exponential growth. Although the correlated clusters were found in [11–13] to grow exponentially with time, the deviations from the exponential might be masked by the monitoring process. We propose that the MQ bandwidth stabilizes because the spectral components located at different areas of the spectrum have different decay rates. In this work, we use developing of our preliminary guess [18] to demonstrate the explicit explanations of results obtained in [11–13].

2 Growth and Decay of the MQ Coherences in Various Processes of the Formation and Degradation of Correlations in Spin Systems

In the conventional MQ NMR spectroscopy, the secular part of the nuclear dipole–dipole interaction (DDI) in a crystal is described by the Hamiltonian [19]

$$H_d = \sum_{i \neq j} b_{ij} S_{zi} S_{zj} - (1/2) \sum_{i \neq j} b_{ij} S_{+i} S_{-j}. \quad (1)$$

The corresponding effective Hamiltonian for the system subjected to the sequence of rf pulses is

$$H_0 = (-1/4) \sum_{i \neq j} b_{ij} (S_{+i} S_{+j} + S_{-i} S_{-j}), \quad (2)$$

where b_{ij} are the DDI constants and $S_{\pm j} = S_{xj} \pm i S_{yj}$. Hamiltonian (2) is nonsecular with respect to the external magnetic field. In the course of so-called "preparation period" of duration $T = N_0 \tau_0$ [or $T = N(\tau_0 + \tau_1)$, Fig. 1], the initial magnetization transforms into various rather complicated TCFs generated by the different products of spin operators entering into Eqs. (1) and (2). The corresponding density matrix is

$$\rho(T) = \exp\{iH_{\text{eff}} T\} \rho_{\text{eq}} \exp\{-iH_{\text{eff}} T\} = \sum_M \rho_M(T). \quad (3)$$

This matrix can be represented as a sum of the off-diagonal elements (ρ_M), where the magnetic quantum number M denotes the order of MQ coherence and specifies its position in the MQ spectrum. In this section, we deal with the Hamiltonian $H_{\text{eff}} = H_0$ defined by Eq. (2), while in the next section, a modified Hamiltonian is used. Usually the arising coherences are marking by a phase shift φ [1–3, 8–13] The respective phase shift is equal to $M\varphi$, where φ is the phase shift of the first-order coherence. The intensity of the M-quantum coherence can be found from the Mth harmonic of the corresponding Fourier series.

We assume that the distribution function for the coherences in the MQ spectrum has the form

$$g_M(T) \propto \exp\left\{ -\left(\frac{M^2}{K(T)} \right)^{\lambda/2} \right\}. \quad (4)$$

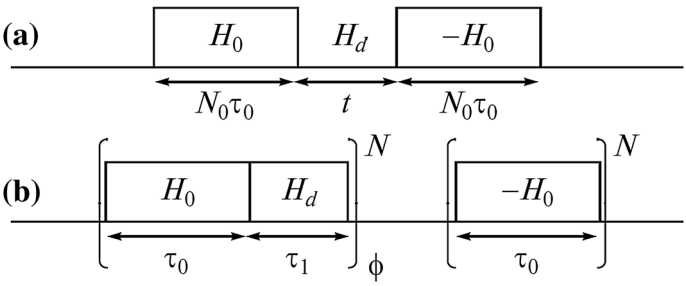

Fig. 1 Schemes of the experiments carried out in **a** [8–10] and **b** [11–13]

For $\lambda = 2$, this expression becomes a Gaussian distribution in M, while for $\lambda = 1$, to the exponential one. The Gaussian form was advanced and justified in [1, 3] for a phenomenological statistical model. This model was applied, e.g., in [1, 8–10] to describe the experimental MQ spectra. By contrast, the authors of [12, 20] argued that, in the description of the coherence distribution, the exponential function is preferable to the Gaussian. The exponential form ($\lambda = 1$) was theoretically examined and substantiated in [6, 21, 22]. The variance $K(T)/2$ in Eq. (4) is determined by the number $K(T)$ of spins dynamically correlated during the preparation time T under the action of Hamiltonian (2). This number, called the number of correlated spins or the effective cluster size, increases with increasing preparation time. The experimental results obtained in [8, 9] for the effective cluster size in adamantane (Fig. 2) show its exponential growth, in good agreement with our theoretical calculations published in [14, 15]; namely,

$$K(T) = \exp(a_0 T), \tag{5}$$

with $a_0 = 0.0083\ \mu s^{-1}$.

For the experimental scheme shown in Fig. 1a [8], the coherence relaxes with time under the action of DDI (1) as [23]

$$\Gamma_{0M}(t) = \exp\{-A^2 M^2 t^2\} \exp\{-Kb^2 t^2/2\}. \tag{6}$$

In Eq. (6), the decay of MQ coherence obeys Gaussian's law with respect to parameter M. This expression was derived in [23] for a situation where each spin in the lattice is surrounded by a large number of the approximately equivalent neighbors.

Following the free-evolution period, a new sequence of pulses inverting the sign of effective Hamiltonian (2) is applied to the system. This is equivalent to the time reversal [1], as a result of which the complicated TCFs (3) again return to its initial

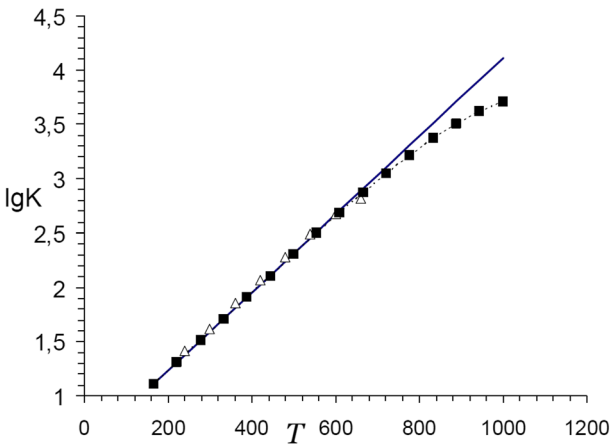

Fig. 2 Common logarithm of the effective cluster size K as a function of the pumping time T (μs) in adamantane. *Triangles* and *black squares* are the experimental results presented in [8] and [9], respectively. The *solid line* is for Eq. (5). The *dashed line* is the result of approximation adopted for the relaxation process considered in [15]

value of the observed quantity corresponding to a zero-quantum longitudinal magnetization. The amplitude of a partial (i.e., for a given value of M) magnetization can be measured by applying $\pi/2$ pulse (to turn the magnetization into the plane perpendicular to an external magnetic field) followed by the Fourier transform with respect to φ. By repeating this procedure many times for various values of t, one can eventually determine the relaxation rate.

For the experimental method schematized in Fig. 1a, the MQ-coherence profile is described by the following function of M and time:

$$f_{0M}(T,t) = \frac{2}{\sqrt{\pi K(T)}} \exp\left\{-\frac{M^2}{K(T)}\right\} \exp\{-A^2M^2t^2\} \exp\{-K(T)b^2t^2/2\}. \quad (7)$$

The constants A^2 and b^2 are the respective lattice sums of the coefficients b_{ij} in Hamiltonian (1). Using the experimental results obtained in [8] for adamantane, we found [23] that in this crystal $A^2 \approx 200$ m s^{-2} for $K = 650$ (Fig. 3).

As in [8–10], we determine the effective cluster size $K_{\text{eff}}(T,t)$ from the half-width of the spectral band. The corresponding intensity profile can be described by introducing the following effective Gaussian distribution over M:

$$\exp\left\{-\frac{M^2}{K_{\text{eff}}(T,t)}\right\} = \exp\left\{-\frac{M^2}{K(T)}\right\} \exp\{-A^2M^2t^2\},$$

with

$$K_{\text{eff}}(T,t) = \frac{1}{1/K(T) + A^2t^2}. \quad (8)$$

The first and the last multipliers in Eq. (7) have no effect on the cluster size because they do not depend on M. These multipliers are responsible only for a change in intensity of the entire spectrum. It follows from Eq. (8) that the width of the MQ spectrum and the effective cluster size $K_{\text{eff}}(T,t)$ both decrease with increasing decay time [i.e., the time of evolution under the action of Hamiltonian (1)], in full agreement with the experimental results obtained in [9].

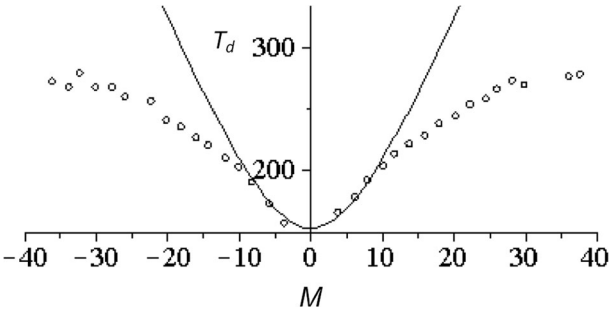

Fig. 3 Decoherence rates $1/T_d$ (in ms^{-1}) for different orders of coherence in the cluster of size $K = 650$ ($T = 660$ μs). The *circles* correspond to the experimental rates [8] and the *curve* is for the function $1/T_d = 205.48M^2 + 23145.1$

3 Growth and Decay of the MQ Coherences in the Processes Including Both Formation and Degradation of the Correlations in Spin Systems

As opposed to the conventional MQ experiments, the experiments performed in [11–13] (Fig. 1b) lead to the substitution of a single Hamiltonian by the new special effective Hamiltonian representing a weighted sum of Hamiltonians (1) and (2):

$$H_{\text{eff}} = (1-p)H_0 + pH_d, \tag{9}$$

with

$$p = \tau_1/\tau_c, \quad \tau_c = \tau_0 + \tau_1.$$

In the preceding approach, Hamiltonians (1) and (2) act separately at different time intervals. Now, both terms in Eq. (9) operate simultaneously, with the first one being responsible for a decrease in the growth rate of coherence, compared to a pure situation with $p = 0$, while the second, for a change in the damping law given by Eq. (7). For a model system comprising 201 equivalent spins, the damping magnitude was numerically evaluated in [24]. It was found in [24] that the damping time is inversely proportional to p and decreases with increasing order of coherence.

The number of spins dynamically correlated during the course of preparation period is specified by the second moment $K(N\tau_c) = 2 << M^2 >>$ of the coherence intensity profile [14, 25]. It is thus of interest to calculate the time dependence of this moment and compare it with the result given by Eq. (5). It was shown in Ref. [18] that for $p << 1$ the second moment increases with time $T = N\tau_c$ as

$$K(T) = \exp(a_p T), \tag{10}$$

where

$$a_p \approx a_0(1-p). \tag{11}$$

If $p << 1$ in the case of simultaneous emergence and degradation of MQ coherences (see Fig. 1b), a coherence that arises at time instant t under the interaction H_0 from Hamiltonian (9) on the time interval $[0, T]$ will further degrade under the interaction pH_d from Hamiltonian (9). Then the decay occurs during a time interval of $T - t$. As it follows from the aforesaid, to describe the degradation in the experiment (Fig. 1b), one has to replace the instant time t by average with respect to the emergence instant of coherence. Thus for a function describing the decay of coherence with a given M, we obtain:

$$\langle \Gamma_M(T-t)\rangle_t = \langle \exp\{-p^2A^2M^2(T-t)^2\}\rangle_t. \tag{12}$$

To carry out averaging in Eq. (12), one needs to know the time-dependent probability density $R(t)$ of coherence emerging. It can be obtained by taking the time derivative of expression (10):

$$R(t) = \frac{1}{D}\frac{dK(t)}{dt} = \frac{a_p}{D}\exp(a_p t), \tag{13}$$

where D is the normalization factor

$$D = \exp(a_p T) - 1.$$

As the result of averaging in Eq. (12), we arrive at the following expression for the TCF describing the intensity relaxation of the Mth-order coherence in the MQ spectrum:

$$\langle \Gamma_M(T-t)\rangle_t = \int_0^T \exp\{-p^2A^2M^2(T-t)^2\}R(t)dt = \frac{U_2(y,m)}{1-e^{-y}}, \tag{14}$$

where $y = a_pT$, $m = |M|\frac{Ap}{a_p}$, and

$$U_2(y,m) = \int_0^y e^{-x}e^{-(mx)^2}dx = \frac{\sqrt{\pi}}{2m}\exp\left(\frac{1}{4m^2}\right)\left[erf\left(ym+\frac{1}{2m}\right) - erf\left(\frac{1}{2m}\right)\right]. \tag{15}$$

Hence, with regard to the relaxation, the MQ spectrum can be written as

$$f_M(T) \propto g_M(T) < \Gamma_M(T-t) >_t. \tag{16}$$

We now define the average effective cluster size $K_{\text{eff}} = M_e^2$ as its value for which the intensity of MQ spectrum is lowered by a factor of e, i.e.,

$$\exp\left\{-\left(\frac{M_e^2}{K(T)}\right)^{\lambda/2}\right\}\frac{U_2(y,m_e)}{1-e^{-y}} = \frac{1}{e}, \tag{17}$$

where $m_e = |M_e|\frac{Ap}{a_p}$. For $y = a_pT << 1$ one has

$$M_e \approx e^{y/2}\left\{1 - \frac{1}{3\lambda}\left(\frac{yAp}{a_p}e^{y/2}\right)^2\right\}.$$

In the limit $y = a_pT >> 1$, K_{eff} achieves its steady-state value

$$K_{\text{st}} \approx \frac{3,2a_p^2}{A^2p^2}. \tag{18}$$

In this work, we solved Eq. (17) numerically with the experimental value of parameter p taken from [12]. The results obtained are shown in Fig. 4.

4 Discussion

The time dependence of the effective number of correlated spins K_{eff} calculated in this work (Fig. 4) is in close agreement with the experimental results obtained in [12]. It adequately reflects all the characteristic features of the observed time evolution of cluster size. The most important results of the theory presented above are the following.

The stabilization of cluster size was experimentally observed in [12], where it was found that the steady-state value K_{st} is inversely proportional to the square of parameter p, as is predicted by formula (18). The experimental and theoretical p-dependences of K_{st} are demonstrated in Fig. 5. However, the experimental value of the coefficient multiplying this function did not coincide exactly with the ratio of

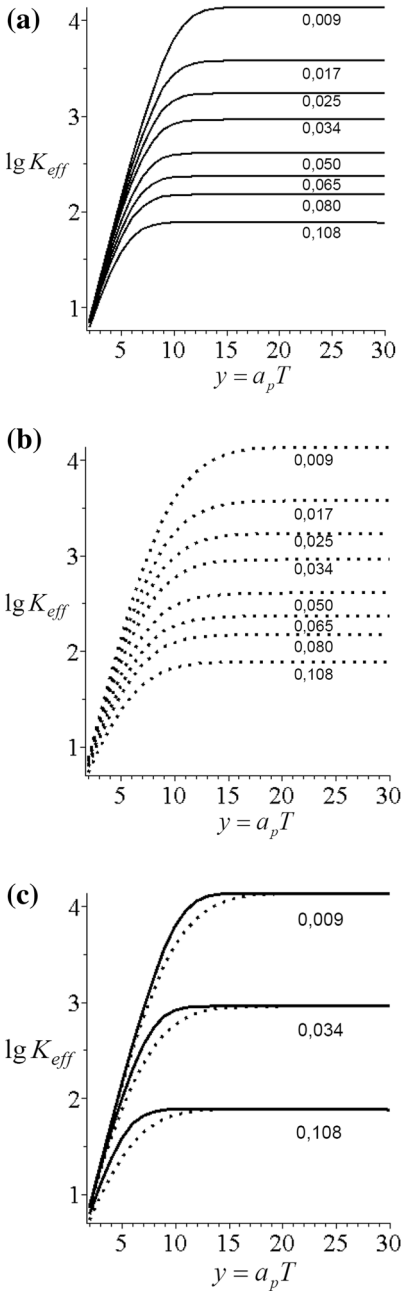

Fig. 4 Evolution of effective cluster size in the experiments schematically illustrated in Fig. 1b (the value of p is indicated under the corresponding curve); **a** for the Gaussian MQ spectrum (4); **b** for the exponential form; and **c** for both forms on the same graph (the Gaussian form is shown by the *solid lines* and the exponential form, by *dots*); the *abscissa* is the time in units of a_p^{-1}

parameters from Eq. (18) that was earlier determined in [15, 23] (cf. Figs. 2, 3). We believe that one possible reason is that in a time ($y \leq 10$) of the experiment conducted in [12] the steady state was not achieved.

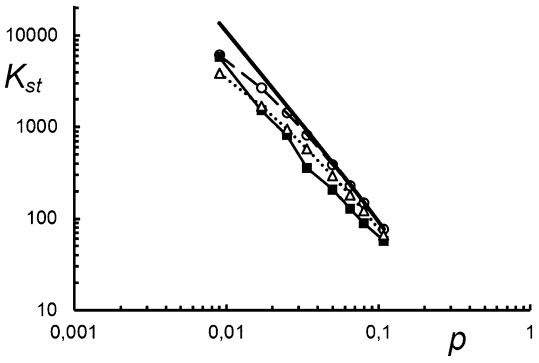

Fig. 5 Stabilized cluster size K_{st} of correlated spins as a function of the perturbation parameter p. The experimental results from [12] are shown by the *black squares*. The data obtained for $y = 10$ (Fig. 4) are indicated by the *circles* for the Gaussian MQ spectrum (4) and by *triangles*, for the exponential form. The data for both forms at $y = 30$ which equal (18) are shown by *solid line*

According to the aforesaid, the stabilization of the cluster size is associated with the behavior of the MQ-coherence profile as a function of M. Indeed, the M-dependence of the MQ spectrum is expressed by

$$f_M(T) = g_M(T) < \Gamma_M(T-t) >_t \propto \exp\left\{-\left(\frac{M^2}{K(T)}\right)^{\lambda/2}\right\} < \exp\{-p^2A^2M^2(T-t)^2\} >_t, \qquad (19)$$

where the number K grows exponentially with T. Therefore, the first factor in Eq. (19) depends on M weaker than the second one, so that the M-dependence of the MQ spectrum is almost completely determined by the latter. In Eqs. (12), (13) and (14), the number of coherences $K(t)$ achieves its maximal value $K(T)$ near the boundary $t = T$. At a distance of $\Delta t = T - t$ from it the number of coherences decays exponentially [$R(t) \sim \exp(-a_p \Delta t)$]. As a result, the main contribution to the integral in Eq. (14) comes from the area $\Delta t \sim 1/a_p << T$ and, hence, $< \Gamma_M(T - t) >_t$ becomes independent of T. Correspondingly, the intensity profile becomes time-independent, as also does the mean cluster size defined by the band half-width, while the cluster, in reality, continues to grow.

On the other hand, the interpretation based on the localization concept suggested in [11–13, 17] seems to be ambiguous. One can present the following arguments against this idea. Suppose that the interaction pH_d is switched on only at the final step of the experiment, i.e., at the stage of evolution reversal, while the correlations have been prepared with the ideal Hamiltonian H_0. From the theoretical viewpoint, this implies a cyclic permutation of the evolution operators under the sign Tr in the expression describing the observed signal:

$$\Gamma_\phi(N\tau_0, N\tau_c) = Tr\{U_0^+ U_{\phi z} U_p S_z U_p^+ U_{\phi z}^+ U_o S_z\} / Tr\{S_z^2\},$$

where $U_p = \exp\{-iN\tau_c(1-p)H_0 - iN\tau_c p H_d\}$, $U_0 = \exp\{-iN\tau_0 H_0\}$, and $U_{\phi z} = \exp\{i\phi S_z\}$ is the operator for the rotation through an angle φ about the z axis. Mathematically, this procedure is the identical transformation. However, due to the fact that, after the permutation, Hamiltonian H_0 is no longer distorted by the perturbation H_d, it is beyond reason to speak about the localization occurring in the

course of the preparation period because the large clusters continue to grow. The fact that the cluster size increases in the absence of the above-mentioned perturbation is also pointed out in other works [1, 8–13].

The clusters are characterized by their parameters such as the number of constituent spins, the quantum numbers, etc. [1, 3, 9, 22, 26]. Should the perturbation be switched on at the second (mixing) step of the process, the clusters differing in these parameters would decay with different rates. The authors of [11–13, 26] assume that the number of spins in cluster (K) is a dominant factor that governs the process of cluster destruction and that the decay rate increases with increasing K. This implies that the large clusters are more fragile than the smaller ones and therefore their size stabilizes at a certain value of K.

By contrast, we demonstrate in this work that it is the coherence order (M) that is of primary importance in the cluster evolution. Namely, the MQ coherences with large M decay faster than the lower-order coherences do, so that the MQ band shape stabilizes well before the number of spins in the cluster ceases to increase. In conclusion, the ultimate answer to this problem calls for further experimental and theoretical investigations.

References

1. J. Baum, M. Munovitz, A.N. Garroway, A. Pines, J. Chem. Phys. **83**, 2015 (1985)
2. R.E. Ernst, G. Bodenhausen, A. Wokaun, *Principles of Nuclear Magnetic Resonance in One and Two Dimensions* (Oxford University Press, Oxford, 1987)
3. M. Munovitz, A. Pines, Adv. Chem. Phys. **6**, 1 (1987)
4. P.K. Wang, J.P. Ansermet, S.L. Rudaz, Z. Wang, S. Shore, C.P. Slichter, J.H. Sinfelt, Science **234**, 35 (1986)
5. J. Baum, A. Pines, J. Am. Chem. Soc. **108**, 7447 (1986)
6. S.I. Doronin, A.V. Fedorova, E.B. Fel'dman, A.I. Zenchuk, J. Chem. Phys. **131**, 104109 (2009)
7. J.A. Jones, Prog. NMR Spectrosc. **59**, 91 (2011)
8. H.G. Krojanski, D. Suter, Phys. Rev. Lett. **93**, 090501 (2004)
9. H.G. Krojanski, D. Suter, Phys. Rev. A **74**, 062319 (2006)
10. G. Cho, P. Cappelaro, D.G. Cory, C. Ramanathan, Phys. Rev. B **74**, 224434 (2006)
11. G.A. Álvarez, D. Suter, Phys. Rev. Lett. **104**, 230403 (2010)
12. G.A. Álvarez, D. Suter, Phys. Rev. A **84**, 012320 (2011)
13. G.A. Álvarez, R. Kaiser, D. Suter, Ann. Phys. (Berlin) **525**, 833 (2013)
14. V.E. Zobov, A.A. Lundin, JETP **103**, 904 (2006)
15. V.E. Zobov, A.A. Lundin, Russ. J. Phys. Chem. B **2**, 676 (2008)
16. V.L. Bodneva, A.A. Lundin, JETP **116**, 1050 (2013)
17. G.A. Álvarez, D. Suter, R. Kaiser, Science **349**, 846 (2015)
18. V.E. Zobov, A.A. Lundin, JETP **113**, 1006 (2011)
19. A. Abragam, *Principles of Nuclear Magnetism* (Oxford University Press, Oxford, 1961)
20. S. Lacelle, S.J. Hwang, B.G. Gerstein, J. Chem. Phys. **99**, 8407 (1993)
21. E.B. Fel'dman, Appl. Magn. Reson. **45**, 797 (2014)
22. A.A. Lundin, V.E. Zobov, JETP **120**, 762 (2015)
23. V.E. Zobov, A.A. Lundin, JETP **112**, 451 (2011)
24. S.I. Doronin, E.B. Fel'dman, A.I. Zenchuk, J. Chem. Phys. **134**, 034102 (2011)
25. A.K. Khitrin, Chem. Phys. Lett. **274**, 217 (1997)
26. C.M. Sánchez, R.H. Acosta, P.R. Levstein, H.M. Pastawski, A.K. Chattah, Phys. Rev. A **90**, 042122 (2014)